Two-photon excited fluorescence enhancement with broadband versus tunable femtosecond laser pulse excitation

Chao Wang
Alvin T. Yeh

Two-photon excited fluorescence enhancement with broadband versus tunable femtosecond laser pulse excitation

Chao Wang and Alvin T. Yeh
Texas A&M University, Department of Biomedical Engineering, 3120 TAMU, College Station, Texas 77843-3120

Abstract. The inverse relationship between two-photon excited fluorescence (TPEF) and laser pulse duration suggests that two-photon microscopy (TPM) performance may be improved by decreasing pulse duration. However, for ultrashort pulses of sub-10 femtosecond (fs) in duration, its spectrum contains the effective gain bandwidth of Ti:Sapphire and its central wavelength is no longer tunable. An experimental study was performed to explore this apparent tradeoff between untuned sub-10 fs transform-limited pulse (TLP) and tunable 140 fs pulse for TPEF. Enhancement factors of 1.6, 6.7, and 5.2 are measured for Indo-1, FITC, and TRITC excited by sub-10 fs TLP compared with 140 fs pulse tuned to the two-photon excitation (TPE) maxima at 730 nm, 800 nm, and 840 nm, respectively. Both degenerate ($v_1 = v_2$) and nondegenerate ($v_1 \neq v_2$) mixing of sub-10 fs TLP spectral components result in its broad second-harmonic (SH) power spectrum and high spectral density, which can effectively compensate for the lack of central wavelength tuning and lead to large overlap with dye TPE spectra for TPEF enhancements. These pulse properties were also exploited for demonstrating its potential applications in multicolor imaging with TPM. © *2012 Society of Photo-Optical Instrumentation Engineers (SPIE).* [DOI: 10.1117/1.JBO.17.2.025003]

Keywords: two-photon excited fluorescence; femtosecond laser pulse; nonlinear optical microscopy.

Paper 11466 received Aug. 29, 2011; revised manuscript received Nov. 7, 2011; accepted for publication Dec. 7, 2011; published online Mar. 2, 2012.

1 Introduction

Two-photon microscopy (TPM), based on ultrafast laser pulse scanning technique, generates nonlinear optical signals from biosamples for rendering high resolution images. TPM is noninvasive and capable of imaging live cells within their extracellular microenvironment deep inside thick tissues. Nonlinear light-matter interactions between near-infrared femtosecond (fs) laser pulse and tissue constituents enable intrinsic optical sectioning,[1–3] high signal-to-background ratio[2] and large depth imaging.[4] The dependence of two-photon signal generation, e.g., two-photon excited fluorescence (TPEF) and second harmonic generation (SHG), on fs-pulse properties, such as pulse shape[5,6] and temporal duration[7–11] suggests that TPM performance may be improved by utilizing shorter pulse durations. However, as the fs-pulse decreases in duration, its spectrum necessarily broadens such that for a sub-10 fs pulse its spectral bandwidth can extend more than 100 nm (if centered at ~800 nm) and its central wavelength is no longer tunable. Given endogenous and exogenous fluorophores with two-photon excitation (TPE) maxima throughout the Ti:Sapphire laser-tuning range, a question arises whether the inability to tune the central wavelength of broadband fs-pulses compromises its utility for TPM compared with tunable narrowband fs-pulses.

Assuming frequency invariant response of dye-molecules to TPE, TPEF yield varies inversely with fs-pulse duration,[7] given identical pulse shapes. A number of studies have characterized this relationship experimentally albeit with subtle but important differences in how the fs-pulse duration was varied. In two of those studies, the fs-pulse duration was varied by introducing dispersion, leading to broadened duration while maintaining the pulse spectrum.[7,8] Results nearly consistent with the inverse proportionality relationship between TPEF yield and fs-pulse duration were reported, but interpretation of these results remains controversial. It can be shown that, for these studies, TPEF yield was actually related to the dispersion effect on fs-pulse rather than the effects of pulse duration on two-photon processes.[10] In other words, the results did not reflect photophysics of two-photon absorption (and subsequent fluorescence) but that of pulse peak-power degradation by group velocity dispersion.

This inverse proportionality relationship between TPEF and pulse duration has also been studied using transform-limited fs-pulses. By using transform-limited pulses, both duration and spectrum change, and thus, for instances of frequency dependent molecular two-photon absorption, TPEF yield was shown to depend on the overlap integral with fs-pulse SH power spectrum.[10] Using a tunable narrowband fs-pulse laser, shorter pulse durations could be obtained by compression of spectrally broadened pulses through optical fibers. With grating compressor and highly nonlinear photonic crystal fibers, TPEF was enhanced when using compressed compared to narrowband fs-pulse,[9,11] and imaging depth with TPM was also extended by using the compressed fs-pulse.[9] For pulses as short as sub-10 fs, its spectrum encompasses the effective gain bandwidth of Ti: Sapphire,[12] thus making its central wavelength untunable. This study was designed to investigate whether gains in TPE utilizing ultrashort pulses were mitigated by its fixed central wavelength compared with tunable narrowband pulses.

Address all correspondence to: Chao Wang, Texas A&M University, Department of Biomedical Engineering, 3120 TAMU, College Station, Texas 77843-3120. Tel: 979-845-8811; Fax: 979-845-4450; E-mail: chaowang9@yahoo.com.

In this research, TPEF yields are measured with three organic dye phantoms excited by nearly transform-limited sub-10 fs (sub-10 fs TLP for simplicity hereafter) and tunable 140 fs pulses. To conduct this proof-of-principle study without loss of generality, Indo-1, FITC, and TRITC were selected for their distinct TPEF characteristics, i.e., TPE spectral peak positions, respectively, located to high-frequency (Indo-1), on spectral peak (FITC), and to low-frequency wing (TRITC) of the sub-10 fs TLP spectrum. By direct comparison and calculation, the physics behind the differentiated TPEF enhancements among the three dye-phantoms is discussed, which evokes further studies on multicolor TPEF enhancements with a mixture of the dye-phantoms, mutual quenching via one-photon absorption (OPA), and associated solvent effect.

This paper is organized as follows: a description of methodology detailed in Sec. 2 includes experimental setup, systematic calibrations, and dye-phantom preparation. Section 3 is devoted to experimental protocol, results presentation, analysis on measured and calculated TPEF enhancements, a semi-quantitative discussion on the differentiated TPEF enhancements, and phantom studies as well as simulations on multicolor TPEF enhancement under environmental influences. Finally, Sec. 4 concludes this paper.

2 Materials and Methods

The integrated experimental setup is shown in Fig. 1(a) and consists of three units: 1. two excitation schemes with group delay dispersion (GDD) compensation, previously optimized with the setup shown in Fig. 1(b) for delivering sub-10 fs TLP in situ (i.e., at the focal spot of the phantom center), 2. dispersion-less laser beam expanding and focusing with parabolic mirrors, and 3. TPEF collection with a custom-designed compound lens well-coupled to a spectrograph. This experimental design ensures delivery of sub-10 fs TLP in situ, high-efficiency fluorescence collection, and good spectral resolution for accurate quantification of TPEF yields. The three dye-phantoms were prepared at 100 μM concentration[7] with Indo-1 (SKU#1-1202, Invitrogen) and FITC (F3651, Sigma-Aldrich) dissolved in deionized water and TRITC (87918, Sigma-Aldrich) in methanol.

2.1 Two Excitation Schemes

A software-controlled tunable Ti:Sapphire laser (pulse duration 140 fs, repetition rate 80 MHz, horizontal linearly-polarized, Chameleon Ultra II, Coherent) is used for TPEF measurements over the tuning range from 700 to 900 nm at 10 nm increments. This tuning range approximates the spectral full-width at tenth-maximum (FWTM: ~190 nm) of sub-10 fs mode-locked pulse from the untuned Ti:Sapphire laser (central-wavelength 792 nm, FWHM ~130 nm, repetition rate 75 MHz, horizontal linearly-polarized, Synergy PRO, Femtolasers). A variable neutral density (ND) filter (spectral window 380 to 1200 nm, Thorlabs) is used for laser power adjustment. The accumulative GDD of cuvette (1.25 mm-thick optical-glass-window, 10.0 mm path-length, 23/G/10, Starna Cells), dye-phantom, and ND filter is assumed negligible for the 140 fs pulse of spectral FWTM less than 9 nm.[7,10] However, for sub-10 fs pulses with more than one order of magnitude broader bandwidth, GDD compensation is essential.

Intrinsic sub-10 fs mode-locked pulse from the untuned laser is characterized by its interferometric autocorrelation (IA) trace measured with an autocorrelator (Femtometer, Femtolasers). IA
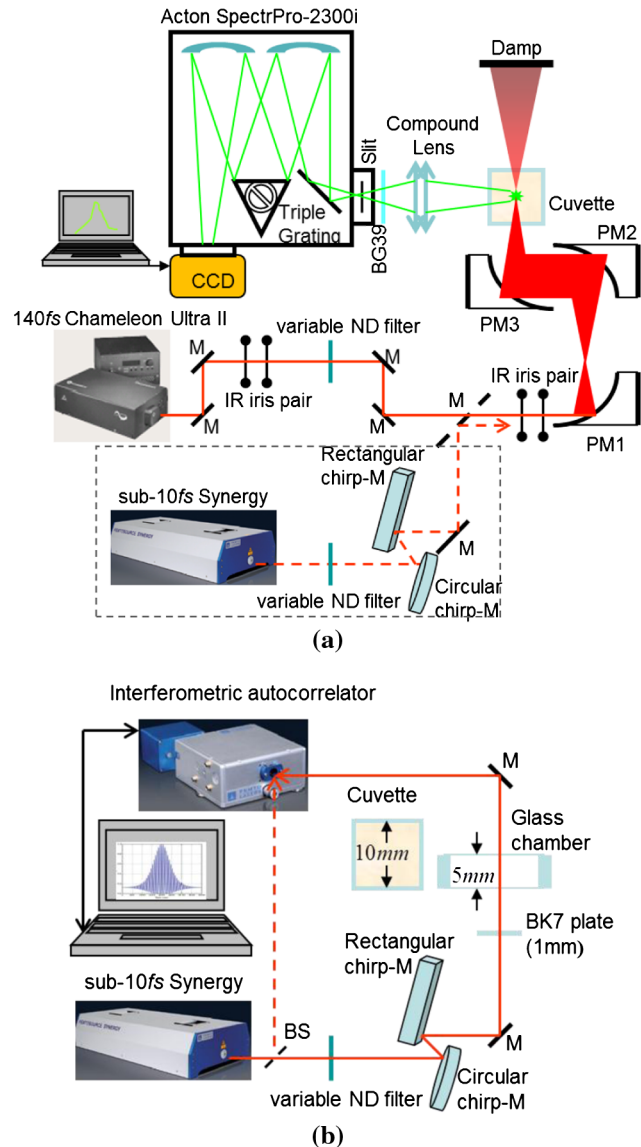

Fig. 1 (a) Experimental configuration for TPEF measurements: PM (parabolic-mirror), ND (neutral density) filter and (b) experimental set up for testing the optimal GDD compensation.

measurement is capable of better resolving fs-pulses because the interferometric fringes contained in IA trace reveal some phase and coherence information about the fs-pulses.[13] GDD compensation for delivery of sub-10 fs TLP in situ was tested with the setup shown in Fig. 1(b), where the ND filter, 1.0 mm BK7 plate, and a home-built 5.0-mm-path-length glass chamber containing dye solution (two 150-μm-thick microscopic cover-glass slices as windows) were added to the beam path upstream of the autocorrelator. The optimal GDD compensation was confirmed by IA trace measurement, i.e., IA trace of the GDD-compensated sub-10 fs TLP in situ shown in Fig. 2(b) agrees well with that of the intrinsic sub-10 fs mode-locked pulse in Fig. 2(a). The optimal GDD compensation was achieved by one pair of light bounces off a rectangular chirp-mirror (GDD/bounce $< -250(\pm 20)$fs^2, GSM201, Femtolasers) and a circular chirp-mirror (GDD/bounce $< -45(\pm 10)$fs^2, GSM001, Femtolasers).
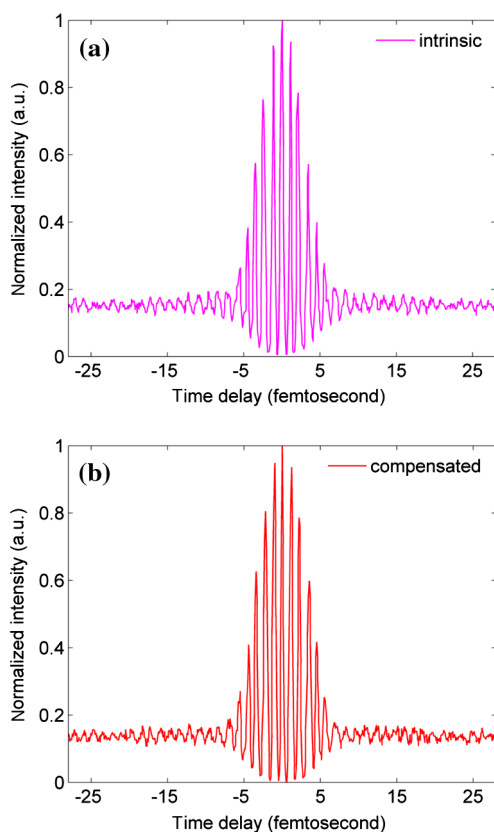
Fig. 2 Interferometric autocorrelation trace of (a) intrinsic sub-10 fs mode-locked pulse from the untuned laser agrees well with that of (b) GDD-compensated sub-10 fs TLP in situ.

2.2 Dispersionless Laser Beam Expanding and Focusing

Dispersionless beam expanding and focusing [recall Fig. 1(a)] is accomplished with three gold-coated 90 deg off-axis parabolic mirrors, i.e., PM1 (effective focal length/EFL, 20.32 mm, 50328AU, Newport), PM2 (EFL 50.8 mm, NT47-098, Edmund Optics), and PM3 (EFL 25.4 mm, NT47-096, Edmund Optics), each of which has a 2-D tilt-adjustment and 3-D linear-translation for accurate alignment. This PM-combination is located at a distance from both laser exit apertures such that the beam size of the tunable 140 fs and untuned sub-10 fs laser beam is ~4 mm. The effective numerical aperture (NA) for beam focusing is ~0.2, corresponding to an estimated[14,15] axial intensity point spread function (IPSF) of ~400 μm by $1/e$ width. This estimated IPSF size in situ is much smaller than cuvette path-length and assumed to be a "point-like source" of fluorescence. Thus, the solid-angle of fluorescence con-beam collection is fixed, which makes TPEF measurements insensitive to slight variations in laser beam size.[7]

2.3 TPEF Collection with a Custom-Designed Compound Lens Coupled to the Spectrograph

A custom-designed compound lens[16,17] was assembled, which consists of two bi-convex lenses in contact (KBX043 with focal-length 19 mm, KBX046 with focal-length 25.4 mm, LKIT-1, Newport); this was to achieve high NA for efficient fluorescence collection and small IPSF projected image onto

the entrance-slit of the spectrograph for high spectral resolution. The resultant compound lens has an EFL of 13.75 mm, effective NA ~0.3, and IPSF projected image size ~147 μm, with the object-distance (51.0 mm from the IPSF in situ to the effective front-principle-point) and image-distance (18.82 mm from the effective back-principle-point to the slit) designed for convenient phantom placement and compound lens adjustment. The lens-tube holder mounted on a triple-stage allowed compound-lens tilt-adjustment and linear-translation. The cuvette-holder was fixed on the optical table to ensure unchanged IPSF position with dye-phantom replacement.

The 300 grooves/mm (BLZ 500 nm) grating was selected in the spectrograph (focal length 300 mm, Acton SpectrPro-2300i, Princeton Instruments), which was well focused onto the CCD camera (1340×100, pixel size 20 μm, PIXIS100, Princeton Instruments). A bandpass filter (spectral window 325 to 620 nm, 3.0-mm-thick, Schott BG39) was attached to the entrance slit to block scattered laser light. With the slit width set at 200 μm (greater than the IPSF projected image size), the achieved spectral resolution was ~1.5 nm.

3 Results and Discussion

TPE and OPA spectra are shown for Indo-1 [Fig. 3(a)], FITC [Fig. 3(b)], and TRITC [Fig. 3(c)]. TPE spectra are acquired by measuring TPEF intensities with 140 fs pulse central wavelength tuned from 700 to 900 nm at 10 nm increments. Indo-1, FITC, and TRITC exhibit TPE maxima at 730, 800, and 840 nm, respectively, which reside to high-frequency, on spectral peak, and to low-frequency of the sub-10 fs TLP spectrum shown in Fig. 3(d). Also shown in Fig. 3(d) are representative 140-fs-pulse spectra centered at 730, 800, and 840 nm, which aptly illustrates differences in spectral bandwidth with the sub-10 fs pulse. By comparing TPE and OPA spectra, it is readily seen that the 140-fs-tuning range, mirroring the FWTM bandwidth of sub-10 fs pulse, excites the dye molecules to TPA-associated final states degenerate with [Indo-1; Fig. 3(a)] and higher in energy [FITC and TRITC; Figs. 3(b) and 3(c)] than OPA-associated 1st-excited singlet state.[18–21] With sub-10 fs TLP of broad FWTM bandwidth, these dye molecule excited states can be simultaneously accessed by degenerate and nondegenerate mixing of the untuned sub-10 fs pulse spectral components, beyond the capability of the narrowband 140 fs pulse. Thus, TPEF enhancement could be expected from greater population of two-photon excited dye-molecules owing to the simultaneous accessibility to TPA-associated final states promoted more readily by sub-10 fs TLP.

Power dependence of TPEF was previously measured for the three dyes to find the suitable excitation power range in which nonresonant TPEF holds.[21] With 140 fs pulse central wavelength tuned to TPE maxima of Indo-1, FITC, and TRITC at 730, 800, and 840 nm, respectively, fluorescence yields were integrated from measured spectra, which are shown on logarithmic plots as a function of excitation power in Fig. 4. For reference, a dash-line of slope 2 is shown to denote the square-law dependence.[7,18] Subtle deviations from the square-law suggest onsets of saturation or higher-order nonlinearities. Power dependence measurements are likewise performed with the untuned sub-10 fs TLP, whose results are shown in Fig. 5. Deviations from the square-law occur for all three dyes at excitation powers above 40 mW. Conservatively, excitation power of 20 mW is used for all TPEF measurements.
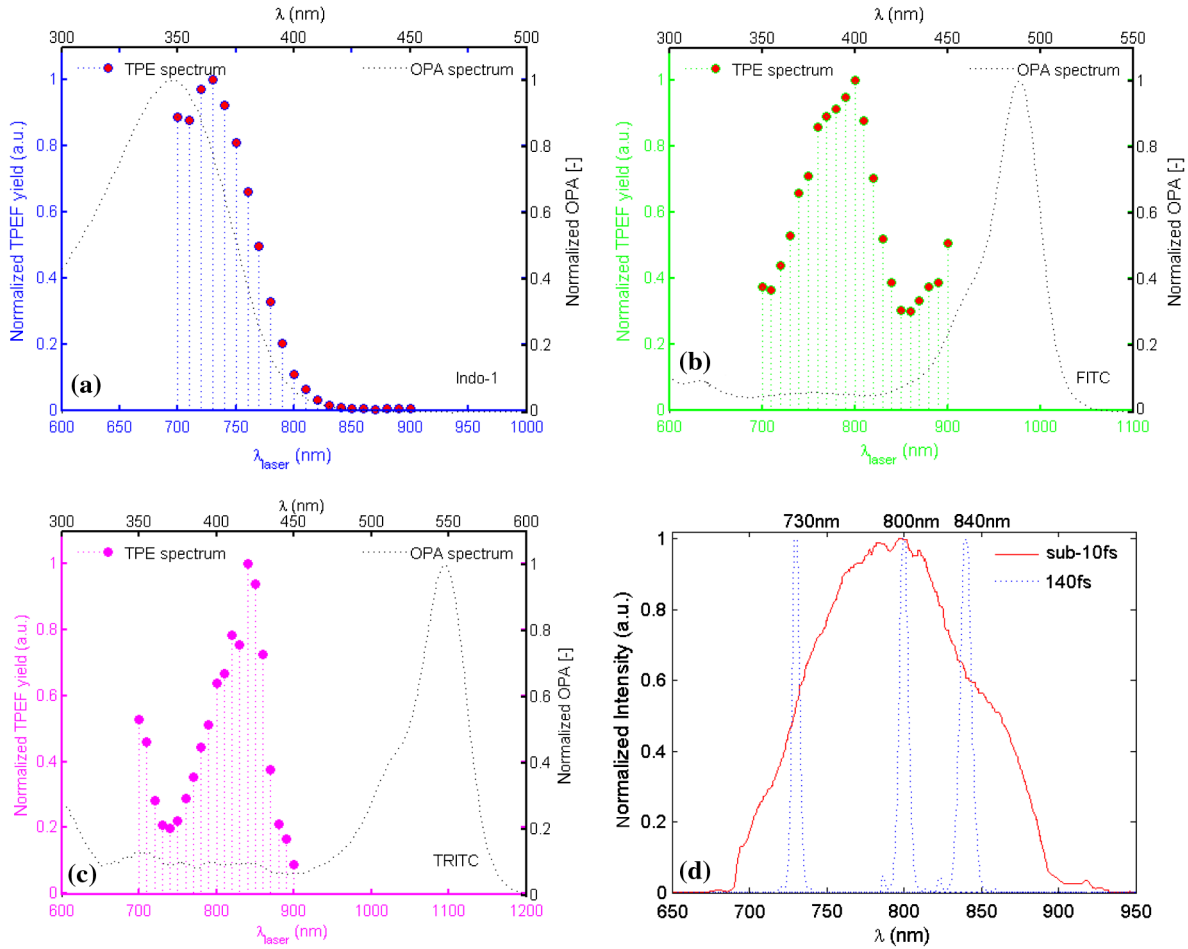
Fig. 3 TPE and OPA spectra of Indo-1 with TPE maximum at 730 nm (a), of FITC with maximum at 800 nm (b), and of TRITC with maximum at 840 nm (c). Laser spectra of the untuned sub-10 fs pulse at 792 nm and 140 fs pulse tuned to 730, 800, and 840 nm (d).

To make direct comparisons of TPEF yields excited with 140 fs and sub-10 fs TLP, all the measured TPEF spectra are normalized to exposure-time for each phantom (5.25, 13.9, and 0.45 sec for Indo-1, FITC, and TRITC, respectively, with 140 fs pulse excitation; 14.5, 10.1, and 0.44 sec for Indo-1, FITC, and TRITC, respectively, with sub-10 fs TLP excitation). 3-D plots are shown in Fig. 6 of normalized TPEF spectra (x and z-axis) for each phantom with respect to 140 fs pulse tuned wavelengths (y-axis; excitation with sub-10 fs TLP at 792 nm). With TPEF yield obtained by integrating the normalized TPEF spectrum, TPEF enhancement is defined as the ratio of TPEF yield excited by the sub-10 fs TLP to that by 140 fs pulse tuned to a specific wavelength. Overall TPEF enhancements readily observed in all three phantoms (Fig. 6) show noticeable advantages of excitation with broadband sub-10 fs TLP over narrowband tunable 140 fs pulse. At TPE maxima for Indo-1, FITC, and TRITC with 140 fs pulse tuned to 730 nm, 800 nm, and 840 nm, respectively, TPEF enhancements of 1.6, 6.7, and 5.2 are measured (summarized in Table 1).

Differentiated TPEF enhancements among the three dye-phantoms suggest that the measured enhancements depend on the overlap between dye TPE and fs-pulse SH power spectra.[22] Assuming dye TPE are proportional with corresponding TPA spectra, TPEF enhancement may be calculated by the ratio of two-photon transition probability (Γ_{TPA}) excited by sub-10 fs versus 140 fs pulse,[7] or,

$$\text{TPEF enhancement} = \frac{[F(t)]_{10\,\text{fs}}}{[F(t)]_{140\,\text{fs}}^{\lambda_{\text{laser}}}}\Bigg|_{\text{measured}}$$

$$\propto \frac{\Gamma_{\text{TPA}}\Big|_{10\,\text{fs}}}{\Gamma_{\text{TPA}}\Big|_{140\,\text{fs}}^{\lambda_{\text{laser}}}}\Bigg|_{\text{calculated}}, \qquad (1)$$

where $[F(t)]$ refers to TPEF yield. Γ_{TPA} is calculated for each dye by the phenomenologically introduced formula,[22] i.e.,

$$\Gamma_{\text{TPA}} = \int_0^\infty g(\omega_0)$$

$$\cdot \left| \int_0^\infty A(\omega_0/2 - \Omega) A(\omega_0/2 + \Omega) d\Omega \right|^2 d\omega_0, \qquad (2)$$

where $g(\omega_0)$ is frequency dependent TPE spectrum of the dye (refer to TPE spectra in Fig. 3), ω_0 denotes two-photon transition energy, $|\int_0^\infty A(\omega_0/2 - \Omega)A(\omega_0/2 + \Omega)d\Omega|^2$ is the fs-pulse SH power spectrum (i.e., two-photon spectral density), $|A|^2$ is the fs-pulse spectrum, and Ω stands for angular frequency of the fs-pulse. Transform-limited pulses are assumed with no phase terms added.
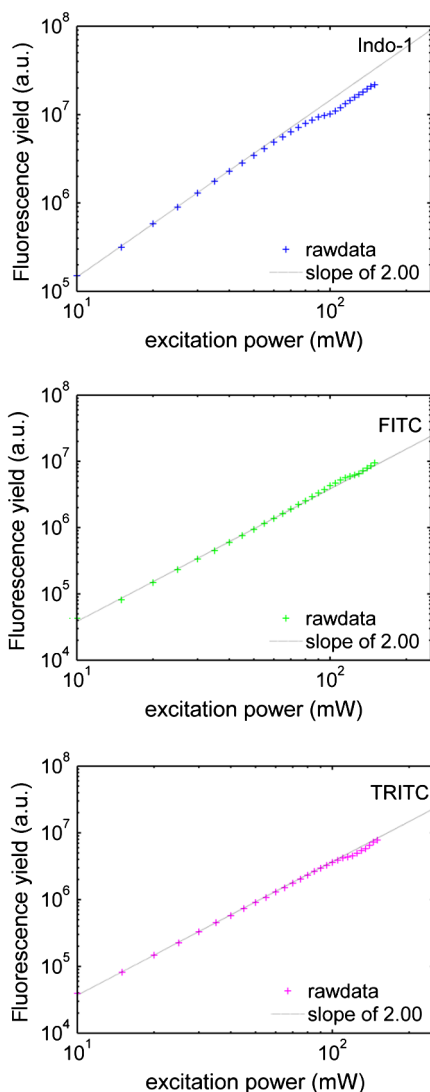
Fig. 4 Logarithmic plots of fluorescence yields versus excitation power (10 to 150 mW at 5 mW increments) with 140 fs pulse tuned to 730, 800, and 840 nm for Indo-1, FITC, and TRITC, respectively. Dashed lines with slope 2 are shown for reference.

Fig. 5 Logarithmic plots of fluorescence yields versus excitation power (10 to 150 mW at 5 mW increments) with sub-10 fs TLP excitation at 792 nm for Indo-1, FITC, and TRITC. Dashed lines with slope 2 are shown for reference.

Calculated TPEF enhancements for Indo-1, FITC, and TRITC with 140 fs pulse tuned to dye TPE maxima at 730, 800, and 840 nm are 3.4, 13.3, and 8.0, respectively. Measured and calculated TPEF enhancements are directly compared in Table 1 and show proportional agreement. This proportional agreement is supportive of the statement that the effective TPEF enhancement depends on the overlap of dye TPE and fs-pulse SH power spectra. Differences between measured and calculated TPEF enhancements (with a reduction factor of 1.5 to 2) may be ascribed to nonidealized experimental conditions including residual phase distortion in the fs-pulse excitations due to imperfect GDD compensation, deviations between dye TPE and two-photon absorption spectra, slight mismatch of laser pulse-repetition-rates, and differences in fluorescence collection efficiencies between two experimental setups.

If frequency invariant response of a dye is assumed, i.e., $g(\omega_0)$ be constant, then the two-photon transition probability, Γ_{TPA}, is proportional to the integral of the fs-pulse SH power spectrum [refer to Eq. (2)]. The integrated SH power spectrum is indicative of TPE capability of the transform-limited fs-pulse.
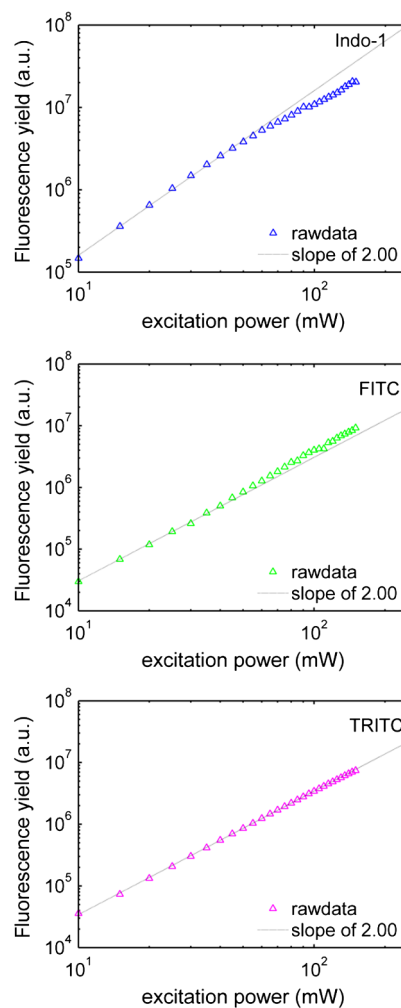
Using measured laser pulse spectra, ratios of sub-10 fs to 140 fs pulse (central wavelength at 730, 800, and 840 nm) integrated SH power spectra are shown in Table 1 with values between 11 and 14. In an idealized case of identical 10 and 140 fs pulse shapes, the ratio of integrated SH power spectra is 14.

Together with our measured and calculated enhancements, these results suggest that optimization of TPEF does not depend solely on central wavelength tuning but ultimately on the overlap of dye TPE and fs-pulse SH power spectra. For ultrashort pulses, TPEF enhancement can be accomplished via broad SH power spectrum and high spectral density which results from both degenerate ($v_1 = v_2$) and nondegenerate ($v_1 \neq v_2$) mixing of pulse spectral components. These SH properties also suggest TPEF enhancements in selective excitation schemes by coherent quantum control of broadband fs-pulse[23–25] relative to narrowband fs-pulse tuning. However, these advantages of broadband fs-pulse excitation may be mitigated in cases where the dye TPE maximum is detuned such that the fs-pulse SH power spectrum overlaps with low absorptive wing (e.g., fluorescent protein variants Venus and DsRed[26]). In addition, parameters such as residual spectral phase and shape can have dramatic effects on the overlap integral[5] in Eq. (2).
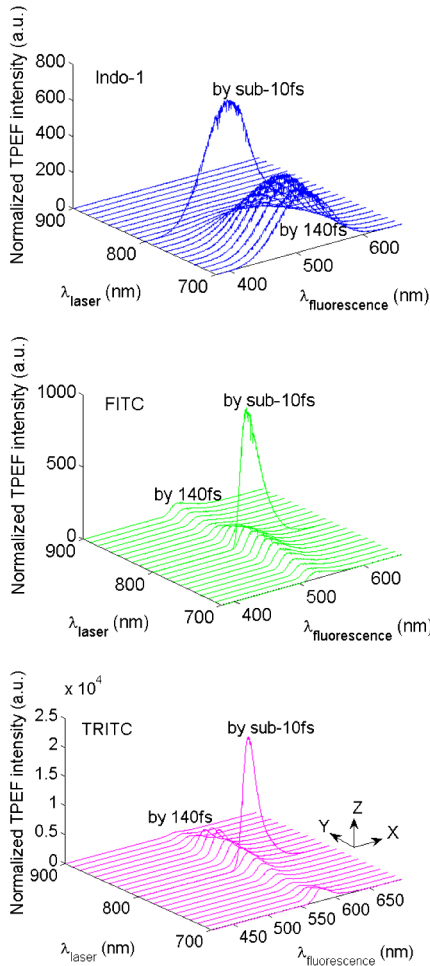
Fig. 6 Normalized TPEF spectra of Indo-1 (peaked at 498 nm), FITC (peaked at 523 nm), and TRITC (peaked at 578 nm) shown in 3-D plots as a function of emission wavelength (x- and z-axis) in relation to laser excitation wavelength of sub-10 fs TLP at 792 nm and 140 fs pulse tuned from 700 to 900 nm at 10 nm increments (y-axis).

Table 1 Measured and calculated TPEF enhancements

Central wavelength of tunable 140 fs pulse	730 nm	800 nm	840 nm
Ratios of integrated SH power spectrum (sub-10 fs pulse : tunable 140 fs pulse)	13.5	12.1	11.3
Organic dye phantoms	Indo-1	FITC	TRITC
Measured TPEF enhancements	1.6	6.7	5.2
Calculated TPEF enhancements	3.4	13.3	8.0

Just as TPEF enhancements are observed in individual dyes with TPE maxima across the sub-10 fs pulse spectrum, the broad SH power spectrum and high spectral density of sub-10 fs TLP suggests an efficient excitation scheme for multicolor TPM applications. To validate this hypothesis, multicolor TPEF enhancements are quantified with a mixture of the three dyes excited by the untuned sub-10 fs TLP and tunable 140 fs
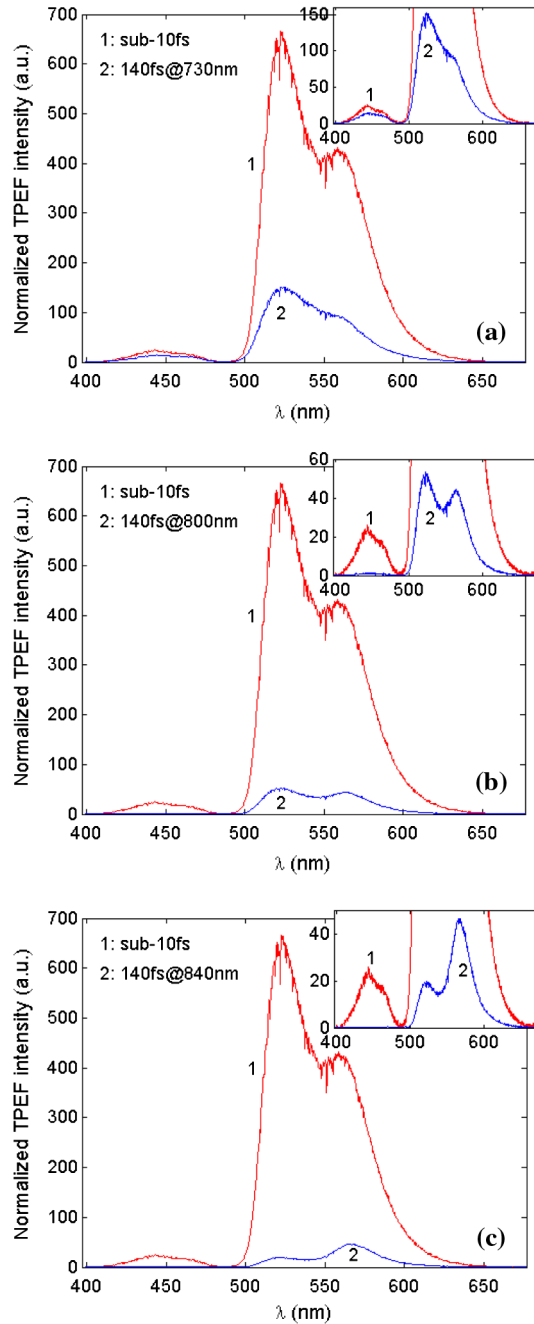
Fig. 7 Normalized mixture TPEF spectrum (Indo-1, FITC, and TRITC) excited by sub-10 fs TLP at 792 nm (red) and by 140 fs pulse (blue) tuned to (a) 730 nm, (b) 800 nm, and (c) 840 nm. Insets show the close-up of the normalized mixture TPEF spectrum excited by 140 fs pulse.

pulse. Individual dye-phantoms (100 μM) of Indo-1, FITC, and TRITC were mixed at the volume ratio of 27:17:1 based on their relative brightness (cf., Fig. 6). TPEF spectra of the mixture are shown in Fig. 7 excited by sub-10 fs TLP and 140 fs pulse tuned to 730 nm [Fig. 7(a)], 800 nm [Fig. 7(b)], and 840 nm [Fig. 7(c)]. Consistent with individual dye TPEF enhancements (recall Fig. 6), multicolor TPEF signals excited by sub-10 fs TLP are overall stronger than those by 140 fs pulse tuned to TPE maxima. The readily achieved enhancement by the untuned broadband fs-pulse would greatly improve discernibility of the generated multicolor TPEF spectrum and

facilitate detectability of multicolor TPM imaging from which post data processing could benefit. This capability of untuned broadband fs-pulse excitation for multicolor TPEF enhancement would not be well recognized without considering extensive overlap of its broad SH power spectrum with the TPE spectra of the constituent dyes in the mixture. In contrast with broadband sub-10 fs TLP excitation, the TPEF spectra of Fig. 7 also show that optimizing the central wavelength of 140 fs pulse for excitation of one dye comes at the expense of degraded
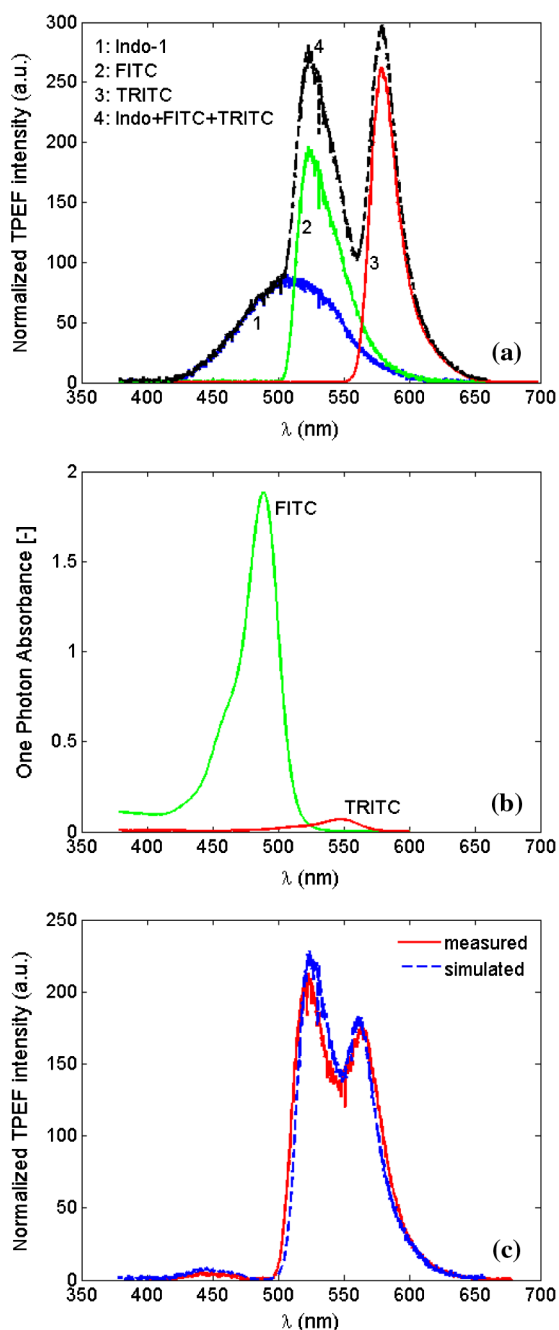
excitation for the others. This observation is particularly acute for Indo-1 with significantly reduced TPEF when excited by 140 fs pulse tuned to 800 nm [Fig. 7(b), inset] and 840 nm [Fig. 7(c), inset].

Nonetheless, multicolor TPEF spectrum of the mixture is not simply a linear summation of individual dye spectra. Individual dye TPEF spectra with sub-10 fs TLP excitation, scaled by the respective volume ratio, and its linear summation are shown in Fig. 8(a). Discrepancies of the summed with the measured mixture TPEF spectra [Fig. 8(c)] are observed particularly with respect to Indo-1 and TRITC spectral peak positions. A number of factors could contribute to this observation, including mutual OPA of TPEF (Ref. 27) and environmental influences (i.e., solvent effects).[28] Measured FITC and TRITC OPA spectra at mixture concentrations are shown in Fig. 8(b) and exhibit significant overlap with Indo-1 and FITC TPEF spectra. In addition, TRITC TPEF exhibited a marked blue-shift and reduction in intensity when dissolved in mixture solvents of water and methanol compared to methanol alone. This blue-shift and reduced intensity is due to some combination of solvent effects[29] and reduced self-quenching.[30] Thus, to simulate the mixture TPEF spectrum, individual Indo-1 and FITC TPEF spectra weighted by their respective mixture volume fraction were summed with TRITC TPEF acquired in (methanol/water) mixture solution. Absorption of mixture TPEF is introduced through Beer's law using measured FITC and TRITC OPA spectra shown in Fig. 8(b) and assuming half the cuvette path-length. The resultant multicolor spectrum by simulation shows good agreement with the measured mixture TPEF spectrum as seen in Fig. 8(c).

These observations illustrate some issues relevant to multicolor TPM imaging, in particular, perturbed TPEF profiles from OPA and environmental effects. However, practical evaluation of environmental influences for TPM imaging should be made with great caution due to their high complexity and entanglement.[28,30] Although imaging depth should be taken into account, frequency dependence of optical scattering and absorption in thick tissue samples can modulate TPEF profiles;[31] however, this effect was not studied here. Implied in our results is the importance of dispersion management especially for broadband fs-pulses to realize the reported enhancements. For TPM using pulses as short as sub-10 fs, dispersion management is nontrivial but has been demonstrated.[32,33]

4 Conclusions

This comparative study highlights some tradeoffs in using broadband versus tunable fs-pulse lasers for TPM. The results are consistent with previous works, which suggest that TPEF can be effectively enhanced by using fs-pulse of shorter durations. However, as fs-pulse duration decreases, its spectral bandwidth increases such that the spectrum of sub-10 fs pulses contains the effective gain bandwidth of Ti:Sapphire and its central wavelength is no longer tunable. Herein, TPEF enhancements are quantified for a series of individual dye phantoms excited by sub-10 fs and 140 fs pulses with TPE maxima across the narrowband fs-pulse tuning range. Measured enhancement factors of 1.6, 6.7, and 5.2 for Indo-1, FITC and TRITC, respectively, are in proportional agreement with theoretical values, owing to the broad SH power spectrum and high spectral density of sub-10 fs TLP. It is believed that these SH properties can effectively compensate for the lack of central wavelength tuning, enabling its larger spectral overlap with dye TPE spectra

Fig. 8 (a) Linear summation (dash-black) and individual TPEF spectra of Indo-1 (blue), FITC (green), and TRITC (red) scaled by mixture volume ratio. (b) Measured OPA spectra of FITC (green) and TRITC (red) at mixture concentrations. (c) Measured (red) and simulated (blue) multicolor TPEF spectra that incorporate OPA contributions from FITC and TRITC and solvent effect plus reduced self-quenching of TRITC.

compared to 140 fs pulse excitation. The advantages of sub-10 fs TLP are also exploited for multicolor TPEF enhancement with a mixture of dyes to demonstrate its potential applications in TPM. Of note are the entangled OPA and solvent effects in interpreting the multicolor TPEF spectrum from the mixture and the compromised excitation scheme with narrowband 140 fs pulse central wavelength tuning. Also, implicit in this study is the essential need for dispersion management of sub-10 fs pulses to realize the enhancements reported and translate to TPM.

References

1. W. R. Zipfel, R. M. Williams, and W. W. Webb, "Nonlinear magic: multiphoton microscopy in the biosciences," *Nat. Biotechnol.* **21**(11), 1369–1377 (2003).
2. P. Theer and W. Denk, "On the fundamental imaging-depth limit in two-photon microscopy," *J. Opt. Soc. Am. A* **23**, 3139–3149 (2006).
3. W. Denk, J. H. Strickler, and W. W. Webb, "Two-photon laser scanning fluorescence microscopy," *Science* **248**, 73–76 (1990).
4. P. Theer, M. T. Hasan, and W. Denk, "Two-photon imaging to a depth of 1000 μm in living brains by use of a Ti:Al$_2$O$_3$ regenerative amplifier," *Opt. Lett.* **28**, 1022–1024 (2003).
5. C. J. Bardeen et al., "Effect of pulse shape on the efficiency of multiphoton processes: implications for biological microscopy," *J. Biomed. Opt.* **4**, 362–367 (1999).
6. V. V. Lozovoy et al., "Applications of ultrashort shaped pulses in microscopy and for controlling chemical reactions," *Chem. Phys.* **350**, 118–124 (2008).
7. C. Xu and W. W. Webb, "Measurement of two-photon excitation cross sections of molecular fluorophores with data from 690 to 1050 nm," *J. Opt. Soc. Am. B* **13**, 481–491 (1996).
8. S. Tang et al., "Effect of pulse duration on two-photon excited fluorescence and second harmonic generation in nonlinear optical microscopy," *J. Biomed. Opt.* **11**(2), 020501-1–020501-3 (2006).
9. G. McConnell, "Improving the penetration depth in multiphoton excitation laser scanning microscopy," *J. Biomed. Opt.* **11**, 054020-1–054020-7 (2006).
10. S. Pang et al., "Beyond the 1/Tp limit: two-photon-excited fluorescence using as short as sub-10-fs," *J. Biomed. Opt.* **14**(5), 054041-1–054041-7 (2009).
11. X. Liang, W. Hu, and L. Fu, "Pulse compression in two-photon excitation fluorescence microscopy," *Opt. Express* **18**(14), 14893–14904 (2010).
12. P. F. Moulton, "Spectroscopic and laser characteristics of Ti:Al$_2$O$_3$," *J. Opt. Soc. Am. B* **3**(1), 125–133 (1986).
13. A. M. Weiner, *Ultrafast Optics*, John Wiley & Sons, Hoboken, NJ (2009).
14. B. Richards and E. Wolf, "Electromagnetic diffraction in optical systems, II. structure of imaging field in an aplanatic system," *Proc. Roy. Soc. London A* **253**(1274), 358–379 (1959).
15. C. J. R. Sheppard and H. J. Matthews, "Imaging in high-aperture optical system," *J. Opt. Soc. Am. A* **4**(8), 1354–1360 (1987).
16. F. A. Jenkins and H. E. White, *Fundamentals of Optics*, 4th ed., McGraw-Hill, New York (1976).
17. R. Kingslake and R. B. Johnson, *Lens Design Fundamentals*, 2nd ed., Academic Press, Elsevier, Burlington, MA (2010).
18. R. W. Boyd, *Nonlinear Optics*, 2nd ed., Academic Press, San Diego, CA (2003).
19. J. W. Lichtman and J. A. Conchello, "Fluorescence microscopy," *Nat. Methods* **2**(12), 910–919 (2005).
20. T. N. Smirnova, E. A. Tikhonov, and M. T. Shpak, "Vibronic structure in the spectra of two-photon absorption of organic dye solutions," *JETP Lett.* **29**(8), 411–414 (1979).
21. Y. R. Shen, *The Principles of Nonlinear Optics*, John Wiley & Sons, New York (1984).
22. D. Meshulach and Y. Silberberg, "Coherent quantum control of multiphoton transitions by shaped ultrashort optical pulses," *Phys. Rev. A* **60**(2), 1287–1292 (1999).
23. T. Brixner et al., "Photoselective adaptive femtosecond quantum control in liquid phase," *Nature* **414**(6859), 57–60 (2001).
24. V. V. Lozovoy and M. Dantus, "Systematic control of nonlinear optical processes using optimally shaped femtosecond pulses," *Chem. Phys. Chem.* **6**(10), 1970–2000 (2005).
25. J. P. Ogilvie et al., "Fourier transform measurement of two-photon excitation spectra: applications to microscopy and optimal control," *Opt. Lett.* **30**(8), 911–913 (2005).
26. H. Hashimoto et al., "Measurement of two-photon excitation spectra of fluorescence proteins with nonlinear Fourier-transform spectroscopy," *Appl. Opt.* **49**(17), 3323–3329 (2010).
27. A. J. Raddosevich et al., "Hyperspectral in vivo two-photon microscopy of intrinsic contrast," *Opt. Lett.* **33**(18), 2164–2166 (2008).
28. A. P. Demchenko et al., "Monitoring biophysical properties of lipid membranes by environmental-sensitive fluorescent probes," *Biophys. J.* **96**(9), 3461–3470 (2009).
29. A. Nag and D. Goswami, "Solvent effect on two-photon absorption and fluorescence of rhodamine dyes," *J. Photochem. Photobiol. A* **206**(2), 188–197 (2009).
30. J. R. Lakowicz, *Principles of Fluorescence Spectroscopy*, 3nd ed., Springer, New York (2006).
31. K. Vishwanath and M. A. Mycek, "Do fluorescence decays remitted from tissues accurately reflect intrinsic fluorescence lifetime?," *Opt. Lett.* **29**(13), 1512–1514 (2004).
32. A. M. Larson and A. T. Yeh, "Ex vivo characterization of sub-10-fs pulses," *Opt. Lett.* **31**(11), 1681–1683 (2006).
33. P. Xi et al., "Two-photon imaging using adaptive phase compensated ultrashort laser pulses," *J. Biomed. Opt.* **14**(1), 014002-1–014002-7 (2009).